

# On the mechanics of tetrakis-like lattices in the stretch-dominated regime



Enrico Babilio<sup>a</sup>, Francesco Fabbrocino<sup>b</sup>, Marc Durand<sup>c</sup>, Fernando Fraternali<sup>d,\*</sup>

<sup>a</sup> Department of Structures for Engineering and Architecture (DiSt), University of Naples Federico II, Via Forno Vecchio, 36, 80134 Naples, Italy

<sup>b</sup> Department of Engineering, Pegaso University, Piazza Trieste e Trento, 48, 80132 Naples, Italy

<sup>c</sup> Matière et Systèmes Complexes (MSC), UMR 7057 CNRS & Université Paris Diderot, 10 rue Alice Domon et Léonie Duquet, 75205 Paris Cedex 13, France

<sup>d</sup> Department of Civil Engineering, University of Salerno, Via Giovanni Paolo II, 132, 84084 Fisciano (SA), Italy

## ARTICLE INFO

### Article history:

Received 14 May 2017

Accepted 9 June 2017

Available online 13 June 2017

### Keywords:

Tetrakis lattices  
Stiffest networks  
Elastic moduli

## ABSTRACT

We derive general conditions for the design of two-dimensional *stiffest elastic networks* with tetrakis-like (or 'Union Jack'-like) topology. Upon generalizing recent results for tetrakis structures composed of two different rod geometries (length and cross-sectional area), we derive the elasticity tensor of a lattice with generalized tetrakis architecture, which is composed of three kinds of rods and generally exhibits anisotropic response. This study is accompanied by an experimental verification of the theoretical prediction for the longitudinal modulus of the lattice. In addition, the introduction of a third rod geometry allows to extend considerably the possible lattice geometries for isotropic, stiffest elastic lattices with tetrakis-like topology. The potential of the analyzed structures as innovative metamaterials featuring extremely high elastic moduli vs. density ratios is highlighted.

© 2017 Elsevier Ltd. All rights reserved.

## 1. Introduction

Recently, there has been a growing interest in the design and fabrication of lattice metamaterials exhibiting a variety of 'extreme' behaviors not found in natural materials. These may include: exceptional strength- and stiffness-to-weight ratios; excellent strain recoverability; very soft and/or very stiff deformation modes; auxetic behavior; phononic band-gaps; sound control ability; negative effective mass density; negative effective stiffness; negative effective refraction index; superlens behavior; and/or localized confined waves, to name some examples (refer, e.g., to [1–10] and references therein).

As a matter of fact, a challenging approach to fill holes in material property charts (relating elastic stiffness and/or strength properties to material density) consists of playing with the microstructure of lattice materials in order to obtain an optimal combination of material and space (voids) at different scales [1]. Lattice metamaterials are structural networks made up of a large number of unit cells, which feature macroscopic length scales much larger than the length scales of the individual rods, and are such that their mesoscopic mechanical properties mainly derive by the geometry

of the microstructure, rather than from the chemical composition of the material. Lightweight and strong lattices with nanoscale features and hierarchical architecture have been recently fabricated through the coating of additively manufactured polymeric scaffolds with metallic or ceramic materials, obtaining ultralight hollow-tube ceramic nanolattices that exhibit ultrastiff properties across more than three orders of magnitude in density [8], and/or ductile-like deformation and recoverability [6]. Attention is increasingly being given to metamaterials that feature geometrical nonlinear behavior, and precompression-tuned response [11–14].

In a recent work, Gurtner and Durand [15] studied the mechanical properties of isotropic networks of elastic rods in the linear elastic regime. As long as the typical dimensions of a junction are the same as the typical rod thickness, the energy cost associated with node deformation can be neglected in comparison with the rod stretching energy. However, no assumption is made on the relative importance of energy cost associated with node deformation and rod bending, so the mechanical response is generally not equivalent to those of pin-jointed structures. On dimensional grounds [1], it is clear that networks deforming primarily through the beam stretching mode are much stiffer than those deforming through the bending mode. However, stiffness still varies significantly among stretch-dominated networks. Only few structures have the peculiarity of deforming through beam stretching rather than bending: most structures will indeed deform primarily through other mechanisms than pure beam stretching. As an illustration, an hexagonal network will deform through beam bending

\* Corresponding author.

E-mail addresses: [enrico.babilio@unina.it](mailto:enrico.babilio@unina.it) (E. Babilio), [francesco.fabbrocino@unipegaso.it](mailto:francesco.fabbrocino@unipegaso.it) (F. Fabbrocino), [marc.durand@univ-paris-diderot.fr](mailto:marc.durand@univ-paris-diderot.fr) (M. Durand), [f.fraternali@unisa.it](mailto:f.fraternali@unisa.it) (F. Fraternali).

mode if the energetic cost of node deformation is relatively much higher, and through node deformation in the opposite limit (which coincides to pin-jointed structures). Gurtner and Durand [15] have demonstrated the existence of *stiffest elastic networks*, which are stiffer than any lattice materials featuring the same symmetry, density and rod elastic properties. These stretch-dominated networks deform in *affine* way down to the heterogeneity scale *under any loading conditions* that are compatible with the linear elastic regime. Their elastic moduli constitute upper-bounds which are identical (3D) or below (2D) the well-known Hashin–Shtrikman (HS) bounds in the low-density limit. Then, these bounds are more precise than the HS bounds, but limited to networks of elastic rods only, while HS bounds apply to any diphasic structures. It is also worth noting that Deshpande et al. [16] have shown that triangulated structures having bars mutually clamped in the joints still exhibit stretching-dominated regime, and the collapse load is dictated mainly by the axial strength of the struts.

In the two-dimensional (2D) case, a special class of stiffest elastic networks is that of structures showing *tetrakis* (or ‘*Union Jack*’) architecture, that is, lattices that tessellate the plane through square modules of right isosceles triangles [17]. By design, these lattices employ rods with two different lengths: one for the horizontal and vertical rods, and one for the diagonal rods. The cross-sectional areas are then adjusted to satisfy isotropic elastic properties [15].

From the fabrication point of view, both stretching-dominated and bending-dominated lattices can be fabricated employing additive-manufacturing technologies. Some examples are given in [18], in which mechanical microarchitected metamaterials made out of highly stretchable elastomers are fabricated through projection micro-stereo-lithography. Available literature results in this area confirm the theoretical findings about the stiffer response of stretch-dominated lattices structure, as compared to structures featuring relevant bending deformation effects at the nodes and within the bars [6,8]. It is noteworthy that the stretching-dominated response survives in cellular structures away from idealized networks with freely hinged joints [19]. The additive manufacturing of lattices featuring rods tapered near the junctions has also been investigated [20,21], with the aim of minimizing bending effects. The role played by mechanical interlocking connections has been studied in [22].

The present Letter presents a multifold generalization of the results obtained by Gurtner and Durand for tetrakis lattices [15]: (i) we derive the elasticity tensor of a tetrakis lattice with arbitrary shape and anisotropic response (Section 2); (ii) we present an experimental validation of the longitudinal elastic modulus predicted by such a theory against laboratory tests on a physical model (Section 2.2); (iii) we derive more general optimality conditions for the achievement of 2D stiffest networks (Section 3), which assume the presence of three different kinds of rods (horizontal, vertical, and diagonal) in the unit cell. The given results allow us to develop general conditions for the achievement of stiffest elastic networks in 2D, and pave the way to the design of stiff and lightweight structures featuring either one dimension much larger than the others (plane strain), or one dimension much smaller than the others (plane stress). These may be e.g. employed to design lightweight and stiff components of aeronautical structures, or next generation facades of tall buildings.

## 2. Anisotropic response of tetrakis-like lattices

Gurtner and Durand focus their study [15] primarily on stiffest elastic networks with isotropic symmetry (see also [23]). In the present work, we initially extend this study by analyzing the existence conditions for anisotropic structures with ‘*tetrakis-like*’ architecture that deform affinely under any loading conditions.

Such lattices tessellate the plane through rectangular –rather than square – modules of right triangles that show arbitrary aspect ratios between horizontal and vertical edges (Fig. 1(a)). Their elementary unit cell (or ‘*building block*’) consists of the hatched region shown in Fig. 1(b), which features at least two axes of geometric symmetry (depending on the  $h_1$  vs.  $h_2$  ratio). The tetrakis lattices studied in [15] are obtained as a special case, by setting  $h_1 = h_2$ , assuming two different cross-sectional areas for the horizontal and vertical elements (first cross section) and the diagonal elements (second cross section), and using the same material for all the rods. We hereafter allow our tetrakis-like lattices to exhibit different materials and cross-section in different rods, and make use of the symbols  $A_k$ ,  $L_k$  and  $E_k$  to respectively denote the cross sectional area, the reference length, and the Young modulus of the  $k$ th rod forming the building block shown in Fig. 1(b), which connects the central node 0 to node  $k$  ( $k = 1, \dots, 8$ ).

Following the work of [15], we look for the structural conditions under which a tetrakis-like architecture deforms affinely down to the microscopic scale, given an arbitrary, homogeneous and infinitesimal deformation of the lattice at the mesoscopic scale. In a first step, we calculate the strain energy that would be associated with such an affine deformation. We describe such a deformation through a displacement field of the form

$$\mathbf{u} = \boldsymbol{\varepsilon} \mathbf{x}, \quad (1)$$

where  $\mathbf{x}$  denotes the position vector, and  $\boldsymbol{\varepsilon}$  denotes the infinitesimal strain matrix with Cartesian components  $\varepsilon_{ij}$  with respect to a frame  $\{0, \mathbf{e}_1, \mathbf{e}_2, \mathbf{e}_3\}$  having the  $\mathbf{e}_1$  and  $\mathbf{e}_2$  unit vectors aligned with horizontal and vertical rods, respectively, and the  $\mathbf{e}_3$  unit vector orthogonal to the lattice plane. It is an easy task to compute the strain energy  $\mathcal{E}_{\mathcal{L}}$  associated to an affine deformation of a tetrakis-like lattice as follows

$$\begin{aligned} \mathcal{E}_{\mathcal{L}} = & \frac{\varepsilon_{11}^2}{2} \left( h_1(E_1 A_1 + E_5 A_5) + \frac{h_1^4}{16h_3^3} \right. \\ & \times (E_2 A_2 + E_4 A_4 + E_6 A_6 + E_8 A_8) \left. \right) \\ & + \frac{\varepsilon_{22}^2}{2} \left( h_2(E_3 A_3 + E_7 A_7) + \frac{h_2^4}{16h_3^3} \right. \\ & \times (E_2 A_2 + E_4 A_4 + E_6 A_6 + E_8 A_8) \left. \right) \\ & + (2\varepsilon_{12}^2 + \varepsilon_{11}\varepsilon_{22}) \frac{h_1^2 h_2^2}{16h_3^3} (E_2 A_2 + E_4 A_4 + E_6 A_6 + E_8 A_8) \\ & + \varepsilon_{12} (h_1^2 \varepsilon_{11} + h_2^2 \varepsilon_{22}) \frac{h_1 h_2}{8h_3} (E_2 A_2 - E_4 A_4 + E_6 A_6 - E_8 A_8). \end{aligned} \quad (2)$$

Let us define the solid volume intercepted by the building block as  $V_{\mathcal{L}} = \sum_k A_k L_k$ , and the solid volume fraction as  $\phi = V_{\mathcal{L}}/V$ , where  $V$  denotes the volume of the building block. The homogenized strain energy density of the lattice is computed as follows

$$\varphi_{\mathcal{L}} = \frac{\mathcal{E}_{\mathcal{L}}}{V} = \phi \frac{\mathcal{E}_{\mathcal{L}}}{V_{\mathcal{L}}}. \quad (3)$$

We now establish the structural properties of the lattice that are compatible with an affine deformation down to the microscopic scale, by enforcing the balance of forces everywhere in the structure. Under affine deformation, forces distributed in the lattice are parallel to the rods, and the balance equation at every node  $k = 1, \dots, 8$  yields:

$$E_i A_i \varepsilon_i = E_{i+4} A_{i+4} \varepsilon_{i+4} \quad i = \{1, \dots, 4\}, \quad (4)$$

where  $\varepsilon_i = \mathbf{e}_{0i} \boldsymbol{\varepsilon} \mathbf{e}_{0i}$  is the extension of rod connecting nodes 0 and  $i$ , and  $\mathbf{e}_{0i}$  its unit tangent vector. Trivially,  $\mathbf{e}_{0i+4} = -\mathbf{e}_{0i}$ ,  $\varepsilon_{i+4} = \varepsilon_i$ ,

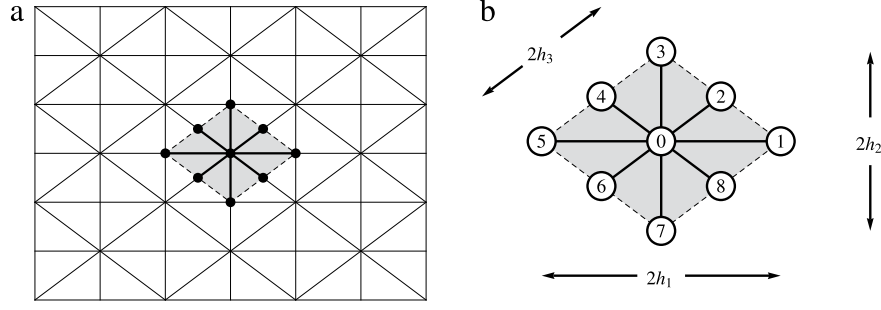


**Fig. 1.** Tetrakis-like lattice and its elementary unit cell (hatched region). The Pythagorean theorem implies  $h_3^2 = (h_1/2)^2 + (h_2/2)^2$ .

and thus, affine deformation requires the following relationships between the elastic stiffness coefficients of the rods forming the building block in Fig. 1(b)

$$E_{i+4}A_{i+4} = E_iA_i \quad i = \{1, \dots, 4\}. \quad (5)$$

It is a trivial task to verify that the balance equation is also satisfied at the central node 0 when Eqs. (5) are satisfied.

The strain energy density of an anisotropic, hyperelastic continuum in 2D is given by (see, e.g., [24,25])

$$\begin{aligned} \varphi_C = & \frac{1}{2} (C_{1111}\varepsilon_{11}^2 + 2C_{1122}\varepsilon_{11}\varepsilon_{22} + C_{2222}\varepsilon_{22}^2) \\ & + 2\varepsilon_{12} (C_{1112}\varepsilon_{11} + C_{1212}\varepsilon_{12} + C_{2212}\varepsilon_{22}). \end{aligned} \quad (6)$$

Comparing term by term Eqs. (3) and (6), and making use of Eqs. (5), we finally obtain the following expressions for the homogenized anisotropic elastic coefficients of a tetrakis-like lattice that deforms affinely under any loading condition:

$$C_{1111} = \frac{\phi h_1 (16h_3^3 E_1 A_1 + h_1^3 (E_2 A_2 + E_4 A_4))}{8h_3^3 V_C}, \quad (7)$$

$$C_{2222} = \frac{\phi h_2 (16h_3^3 E_3 A_3 + h_2^3 (E_2 A_2 + E_4 A_4))}{8h_3^3 V_C}, \quad (8)$$

$$C_{1212} = C_{1122} = \frac{\phi h_1^2 h_2^2 (E_2 A_2 + E_4 A_4)}{8h_3^3 V_C}, \quad (9)$$

$$C_{1112} = \frac{\phi h_1^3 h_2 (E_2 A_2 - E_4 A_4)}{8h_3^3 V_C}, \quad (10)$$

$$C_{2212} = \frac{\phi h_1 h_2^3 (E_2 A_2 - E_4 A_4)}{8h_3^3 V_C}. \quad (11)$$

It is interesting to observe that as a consequence of Eq. (5), the elastic coefficients  $C_{1212}$  and  $C_{1122}$  are equals. Indeed, under affine deformation, forces acting on junctions are oriented along the rods (“axial interactions”) and we recover the Cauchy relation for 2D materials [26]. Eqs. (10)–(11) also show that  $C_{1112}$  and  $C_{2212}$  are related to the geometry of the elementary unit cell of tetrakis-like lattices through:

$$\frac{C_{1112}}{h_1^2} = \frac{C_{2212}}{h_2^2}, \quad (12)$$

reducing the number of independent elastic coefficients to 4.

Let us investigate the sign of the elastic coefficients  $C_{1112}$  and  $C_{2212}$ , by introducing the following dimensionless ratios

$$r_i = \frac{E_i A_i}{E_4 A_4}, \quad i = \{1, 2, 3\} \quad (13)$$

and observing that it results

$$C_{1112}, C_{2212} \begin{cases} > 0, & \text{for } r_2 > 1 \\ = 0, & \text{for } r_2 = 1 \\ < 0, & \text{for } r_2 < 1 \end{cases}. \quad (14)$$

We close the present section by providing the elasticity matrix of anisotropic tetrakis-like lattices in Voigt's notation (refer, e.g. to [26]), which reads

$$\hat{\mathbf{C}} = \begin{pmatrix} C_{1111} & C_{1122} & C_{1112} \\ & C_{2222} & C_{2212} \\ \text{Sym.} & & C_{1212} \end{pmatrix}. \quad (15)$$

A special anisotropic case is that of a lattice whose elasticity matrix (15) is invariant under rotations of the reference frame of an angle  $\pi$  about  $\mathbf{e}_3$  (orthotropic response in the lattice plane, see, e.g., [25]). It is an easy task to verify that such a condition is matched when it results  $C_{1122} = C_{1212} = 0$  i.e., for  $E_2 A_2 = E_4 A_4$  (cf. Eq. (14)). In terms of homogenized engineering elastic constants, namely Young moduli  $\hat{E}_{ii}$ , Poisson ratios  $\hat{\nu}_{ij}$  ( $i, j = 1, 2$ ), and shear modulus  $\hat{G}_{12}$ , it results (see [27])

$$\begin{aligned} \hat{E}_{11} &= \frac{C_{1111}C_{2222} - C_{1122}^2}{C_{2222}} \\ &= \frac{2h_1\phi(h_2^3 E_1 A_1 E_2 A_2 + A_3(8h_3^3 E_1 A_1 + h_1^3 E_2 A_2)E_3)}{V_C (h_2^3 E_2 A_2 + 8h_3^3 E_3 A_3)}, \end{aligned} \quad (16)$$

$$\begin{aligned} \hat{E}_{22} &= \frac{C_{1111}C_{2222} - C_{1122}^2}{C_{1111}} \\ &= \frac{2h_2\phi(h_2^3 E_1 A_1 E_2 A_2 + A_3(8h_3^3 E_1 A_1 + h_1^3 E_2 A_2)E_3)}{V_C (h_1^3 E_2 A_2 + 8h_3^3 E_1 A_1)}, \end{aligned} \quad (17)$$

$$\hat{\nu}_{21} = \frac{C_{1122}}{C_{1111}} = \frac{h_1 h_2^2 E_2 A_2}{8h_3^3 E_1 A_1 + h_1^3 E_2 A_2}, \quad (18)$$

$$\hat{\nu}_{12} = \frac{C_{1122}}{C_{2222}} = \frac{h_1^2 h_2 E_2 A_2}{8h_3^3 E_3 A_3 + h_2^3 E_2 A_2}, \quad (19)$$

$$\hat{G}_{12} = C_{1212} = \frac{h_1^2 h_2^2 \phi E_2 A_2}{4h_3^3 V_C}. \quad (20)$$

The stiffest isotropic elastic networks analyzed in [15] exhibit Young modulus  $\hat{E} = \phi E_0/3$ , shear modulus  $\hat{G} = \phi E_0/8$  and Poisson ratio  $\hat{\nu} = 1/3$ , where  $E_0$  denotes the Young modulus of the rods' material, which is supposed to be equal from rod to rod (see also Section 3). We observe that a tetrakis-like lattice with orthotropic symmetry can achieve directional Young moduli greater than the isotropic value  $\phi E_0/3$ , by properly adjusting the geometry and the stiffness coefficients of the rods. As an example, let us consider a square lattice ( $h_1 = h_2$ ) made out of a single material with Young modulus  $E_0$ , as in [15]. Upon setting

$$\begin{aligned} A_2 < \sqrt{2} A_3 \quad \text{and} \quad \frac{A_3}{2} + \frac{A_2(\sqrt{2} A_2 + A_3)}{2(A_2 + 2\sqrt{2} A_3)} \\ < A_1 < A_3 + \frac{\sqrt{16A_3^2 - 6A_2^2} - \sqrt{2} A_2}{4} \end{aligned} \quad (21)$$

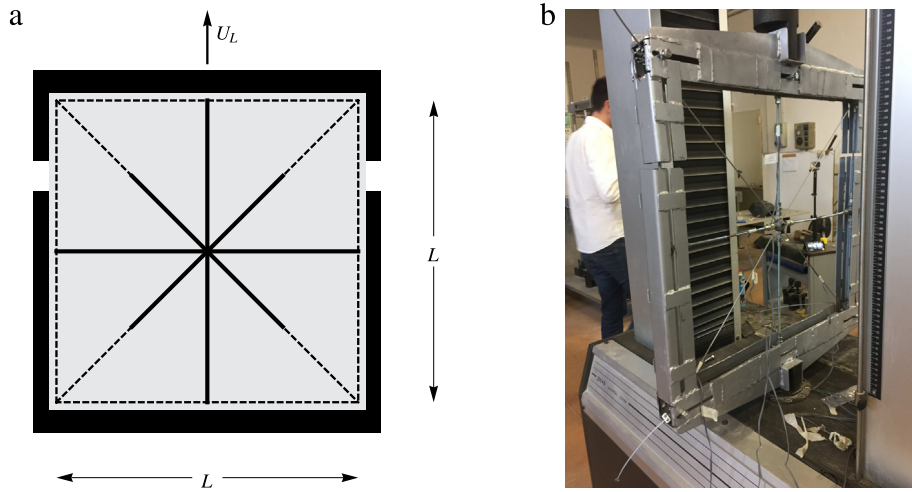


**Fig. 2.** The experimental setup: (a) sketch showing the elementary unit cell of a tetrakis-like lattice (central solid lines) superimposed to the layout of the tested specimen (dashed lines); (b) photograph of the specimen under testing.

it is easily shown that it results

$$\hat{E}_{11} > \frac{\phi E_0}{3}, \quad \hat{E}_{22} > \frac{\phi E_0}{3} \quad (22)$$

although it must be accepted

$$\hat{\nu}_{12} < \frac{1}{3}, \quad \hat{\nu}_{21} < \frac{1}{3}, \quad \hat{G}_{12} < \frac{\phi E_0}{8}. \quad (23)$$

### 2.1. Limitations on the anisotropic elastic coefficients

The stability of the material in its natural state (refer, e.g., to [24,25]) imposes conditions on the elastic coefficients (or *elasticities*) in Eqs. (7)–(11), namely

$$C_{1111} > 0, \quad C_{2222} > 0, \quad C_{1212} > 0, \quad (24)$$

$$C_{1122}^2 < C_{1111}C_{2222}, \quad C_{2212}^2 < C_{1212}C_{2222}, \\ C_{1112}^2 < C_{1111}C_{1212}, \quad (25)$$

$$C_{1122}^2 C_{1212} + C_{1111} C_{2212}^2 + C_{1112}^2 C_{2222} < 2C_{1112} C_{1122} C_{2212} \\ + C_{1111} C_{1212} C_{2222}. \quad (26)$$

By inspecting Eqs. (7)–(9), we immediately verify that our predictions of the elastic coefficients of anisotropic tetrakis-like lattices match the inequalities (24). On the other hand, by taking into account Eqs. (7)–(11), conditions (25) are easily reduced to the equivalent limitations

$$E_3 A_3 (E_2 A_2 + E_4 A_4) h_1^3 + E_1 A_1 (E_2 A_2 + E_4 A_4) h_2^3 \\ + 16 E_1 A_1 E_3 A_3 h_3^3 > 0, \quad (27)$$

$$E_2 A_2 E_4 A_4 h_2^3 + 4 E_3 A_3 (E_2 A_2 + E_4 A_4) h_3^3 > 0, \quad (28)$$

$$E_2 A_2 E_4 A_4 h_1^3 + 4 E_1 A_1 (E_2 A_2 + E_4 A_4) h_3^3 > 0, \quad (29)$$

and similarly Eq. (26) is rewritten as

$$E_2 A_2 E_4 A_4 (E_1 A_1 h_2^3 + E_3 A_3 h_1^3) + 4 E_1 A_1 E_3 A_3 (E_2 A_2 + E_4 A_4) h_3^3 \\ > 0, \quad (30)$$

which trivially turn out to be always true.

### 2.2. Experimental verification of the theoretical prediction for the longitudinal modulus

We carried out an experimental verification of the theoretical prediction (8) for the longitudinal modulus  $C_{2222}$  by running an unidirectional tension test under zero lateral strain on the module of a square tetrakis lattice shown in Fig. 2(a). The central horizontal and vertical rods of the tested specimen consist of M6 threaded bars made out of white zinc plated grade 8.8 steel (DIN 976-1), with nominal cross sectional area  $A_1 = A_3 = 20.10 \text{ mm}^2$ . The perimeter rods are instead made of M4 threaded bars with nominal area of  $8.78 \text{ mm}^2$ . The Young moduli of the above bars are  $E_1 = E_3 = 206 \text{ kN mm}^{-2}$ . The diagonals consist of standard galvanized steel wire ropes formed by 72 wires (EN 10244-2) with nominal cross sectional area  $A_2 = A_4 = 3.073 \text{ mm}^2$  and Young modulus  $E_2 = E_4 = 196 \text{ kN mm}^{-2}$  (all the above properties refer to manufacturer's data). It is worth noting that it results  $(E_2 A_2)/(E_1 A_1) = 0.145$  in the examined structure, while the optimality condition for a stiffest isotropic network implies that the same ratio is equal to  $\sqrt{2}$  [15].

In order to enforce zero lateral strain, the specimen shown in Fig. 2(a) was framed by a steel structure, made of two U-shaped profiles (see Fig. 2(b)). Such profiles were allowed to freely move with respect one another in the vertical direction, while preventing lateral deformation. Hinged connections ensure that the structure deforms in stretching mode, while the high rigidity of the confinement frame guarantees that the deformation of such a structure is negligible as compared to that of the tetrakis lattice.

Fig. 3 shows the force  $F$  vs. longitudinal strain  $\varepsilon$  plot recorded during the test. The longitudinal strain was measured through a strain gauge applied on the central vertical bar, with properties shown in Table 1. The solid straight line appearing in the plot of Fig. 3 provides the least-squares linear fit  $F = fL\varepsilon$  to experimental data, with  $f = 12.4 \text{ kN mm}^{-2}$  and  $L = 660 \text{ mm}$  the specimen length (Fig. 2(a)).

Introducing  $V^*$ , the volume of the parallelepiped domain containing the structure under testing (cf. Fig. 1(b)):

$$V^* = 2V = 2 \frac{V_L}{\phi}, \quad (31)$$

the strain energy density corresponding to the experimental data can be written as follows

$$\varphi_{\text{exp}} = \frac{1}{2} \sigma \varepsilon = \frac{1}{2} \frac{FL}{V^*} \varepsilon = \frac{1}{4} \frac{fL^2 \phi}{V_L} \varepsilon^2 = \frac{1}{2} C_{2222}^{(\text{exp})} \varepsilon^2, \quad (32)$$

**Table 1**  
Characteristics of the strain gauges by Luchsinger, type FLA 3 11 3LT, which employ Cu–Ni alloy foils for the grid and epoxy resin for the backing.

Gauge length (mm)	Gauge width (mm)	Backing length (mm)	Backing width (mm)	Resistance ( $\Omega$ )
3	1.7	8.8	3.5	120

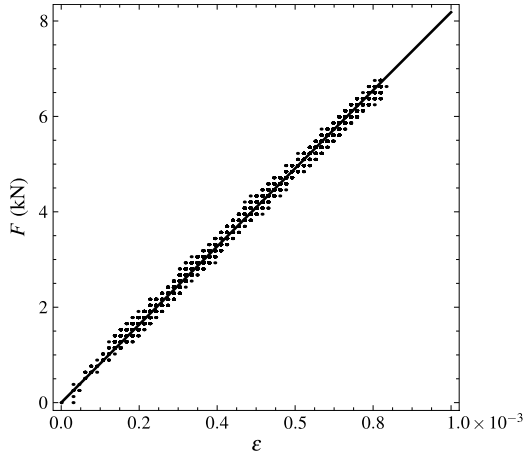


**Fig. 3.** Experimental data and least square fit for the longitudinal modulus.

where  $C_{2222}^{(\text{exp})}$  is the experimental value of the longitudinal modulus to be compared with the theoretical prediction  $C_{2222}^{(\text{th})}$  given by Eq. (8). Making use of the numerical data in Eqs. (8) and (32), we obtain

$$C_{2222}^{(\text{th})} = 97.73 \phi \text{ kNmm}^{-2}, \quad C_{2222}^{(\text{exp})} = 91.86 \phi \text{ kNmm}^{-2} \quad (33)$$

with a theory vs. experiment mismatch of about 6%, which is reasonably acceptable for most engineering applications.

### 3. The isotropic case

Isotropic tetrakis-like lattices are obtained as a special case of the orthotropic lattices analyzed in Section 2, by requiring  $C_{1111} = C_{2222} = C_{1122} + 2C_{1212} (= 3C_{1122})$ , which implies invariance of the elasticity matrix (15) under arbitrary rotations of the reference frame about  $\mathbf{e}_3$  [25]. Making use of Eqs. (7)–(9) we obtain the following requirements for isotropic response of a tetrakis-like lattice

$$A_2 = \frac{A_1 E_1}{h_1 E_2} \frac{8h_3^3}{3h_2^2 - h_1^2}, \quad A_3 = \frac{A_1 E_1}{h_1 E_3} \frac{h_2(3h_1^2 - h_2^2)}{3h_2^2 - h_1^2}. \quad (34)$$

In order for  $A_2$  and  $A_3$  to be both positive in Eqs. (34), the inequality

$$\frac{h_1}{\sqrt{3}} < h_2 < h_1\sqrt{3}, \quad (35)$$

must hold, giving rise to the feasibility region for isotropic response that is hatched in Fig. 4. It is worth noting that Eqs. (34) reduce to  $E_2 A_2 = \sqrt{2} E_1 A_1$  and  $E_3 A_3 = E_1 A_1$  when  $h_1 = h_2$ , i.e., in the case of a square tetrakis lattice [15].

For a lattice made out of a single material with Young modulus  $E_0$ , the substitution of Eqs. (34) into Eqs. (7)–(9) yields

$$\hat{\lambda} = \hat{\mu} = \hat{G} = \frac{E_0 \phi}{8} \quad \hat{M} = \frac{3E_0 \phi}{8}, \quad \hat{E} = \frac{E_0 \phi}{3}, \quad \hat{\nu} = \frac{1}{3} \quad (36)$$

where we have introduced the homogenized Lamé constants  $\hat{\mu} = C_{1212}$  and  $\hat{\lambda} = C_{1122}$ , and the homogenized longitudinal modulus  $\hat{M} = C_{1111} = C_{2222} = \hat{\lambda} + 2\hat{\mu}$ . We recover the values obtained by Gurtner and Durand [15], but the validity of Eqs. (36) is here

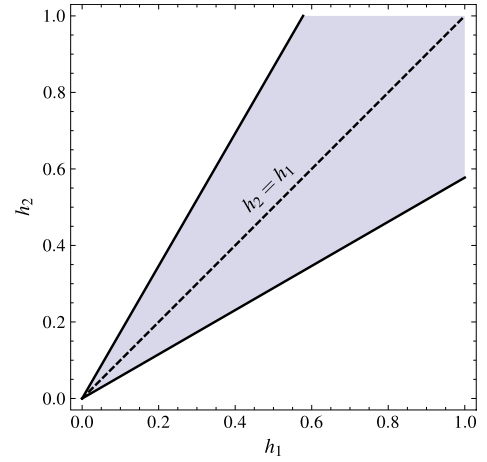


**Fig. 4.** Admissible values of the  $h_2/h_1$  ratio for isotropic response of tetrakis-like lattices.

generalized to the wider feasibility region of isotropic response of tetrakis-like lattices that is illustrated in Fig. 4.

### 4. Concluding remarks

We have generalized the results presented by Gurtner and Durand in [15] for stiffest isotropic elastic networks in 2D, by analyzing a new class of networks based on tetrakis-like lattices. Such lattices feature three different kinds of rods: horizontal, vertical and diagonal, as opposed to the two different kinds of rods of the square tetrakis lattices analyzed in [15]. We have shown that tetrakis-like lattices may exhibit the highest elastic moduli achievable by isotropic lattice materials in 2D, under more general geometry and material conditions, as compared to standard tetrakis lattices (Section 3).

We have also examined the anisotropic response of tetrakis-like lattices that match affinity and equilibrium conditions. Such a study has been complemented by an experimental verification of the theoretical prediction for the longitudinal modulus, which has shown rather good theory-experiment matching. By specializing the anisotropic study to the case of orthotropic lattices, we have proved that is possible to achieve directional Young moduli higher than the upper bound relative to the isotropic case, through a suitable design of the aspect ratio of the unit cell and rods' properties (Section 2). Such a noticeable result paves the way to future studies dealing with the optimal design of anisotropic lattices matching optimal properties along preferred directions. Additional future research lines may regard studies on the effects of suitable initial states of self-stress on the tangent elastic response of lattice materials, as well as investigations on novel additive manufacturing techniques for the realization of prototypes of the designed meta-materials, with special focus on rapid prototyping techniques using materials with different coefficients of thermal expansion and/or swelling materials [28], in order to create internal pre-stress.

### Acknowledgments

The authors wish to thank Geminiano Mancusi, Giuseppe Picentino and Francesco Nunziata (Department of Civil Engineering,

University of Salerno) for their helpful assistance with the experimental part of the present work.

### Compliance with ethical standards

The authors declare that they have no conflict of interest.

### References

- [1] N.A. Fleck, V.S. Deshpande, M.F. Ashby, Micro-architected materials: past, present and future, *Proc. R. Soc. Lond. Ser. A Math. Phys. Eng. Sci.* 466 (2121) (2010) 2495–2516.
- [2] D. Ngo, F. Fraternali, C. Daraio, Highly nonlinear solitary wave propagation in Y-shaped granular crystals with variable branch angles, *Phys. Rev. E* 85 (2012) 036602-1–10.
- [3] Y. Chen, L. Wang, Harnessing structural hierarchy to design stiff and lightweight phononic crystals, *Extreme Mech. Lett.* 9 (2016) 91–96.
- [4] S. Kroedel, N. Thome, C. Daraio, Wide band-gap seismic metastructures, *Extreme Mech. Lett.* 4 (2015) 111–117.
- [5] D. Restrepo, N.D. Mankame, P.D. Zavattieri, Phase transforming cellular materials, *Extreme Mech. Lett.* 4 (2015) 52–60.
- [6] L.R. Meza, S. Das, J.R. Greer, Strong, lightweight, and recoverable three-dimensional ceramic nanolattices, *Science* 345 (6202) (2014) 1322–1326.
- [7] J.J. do Rosario, J.B. Berger, E.T. Lilleodden, R.M. McMeeking, G.A. Schneider, The stiffness and strength of metamaterials based on the inverse opal architecture, *Extreme Mech. Lett.* 12 (2017) 86–96.
- [8] X. Zheng, H. Lee, T.H. Weisgraber, M. Shusteff, J. DeOtte, E.B. Duoss, J.D. Kuntz, M.M. Biener, Q. Ge, Q.J.A. Jackson, S.O. Kucheyev, N.X. Fang, C.M. Spadaccini, Ultralight, ultrastiff mechanical metamaterials, *Science* 344 (6190) (2014) 1373–1377.
- [9] L. Dong, S. Agnew, H. Wadley, Ni bonded TiC cermet pyramidal lattice structures, *Extreme Mech. Lett.* 10 (2017) 2–14.
- [10] Y. Tang, J. Yin, Design of cut unit geometry in hierarchical kirigami-based auxetic metamaterials for high stretchability and compressibility, *Extreme Mech. Lett.* 12 (2017) 77–85.
- [11] A. Amendola, G. Carpentieri, M. de Oliveira, R.E. Skelton, F. Fraternali, Experimental investigation of the softening-stiffening response of tensegrity prisms under compressive loading, *Compos. Struct.* 117 (2014) 234–243.
- [12] A. Amendola, E.H. Nava, R. Goodall, I. Todd, R.E. Skelton, F. Fraternali, On the additive manufacturing, post-tensioning and testing of bi-material tensegrity structures, *Compos. Struct.* 131 (2015) 66–71.
- [13] F. Fraternali, G. Carpentieri, A. Amendola, On the mechanical modeling of the extreme softening/stiffening response of axially loaded tensegrity prisms, *J. Mech. Phys. Solids* 74 (2015) 136–157.
- [14] M.P. O'Donnell, P.M. Weaver, A. Pirrera, Can tailored non-linearity of hierarchical structures inform future material development? *Extreme Mech. Lett.* 7 (2016) 1–9.
- [15] G. Gurtner, M. Durand, Stiffest elastic networks, *Proc. R. Soc. Lond. Ser. A Math. Phys. Eng. Sci.* 470 (2164) (2014) 20130611.
- [16] V.S. Deshpande, M.F. Ashby, N.A. Fleck, Foam topology bending versus stretching dominated architectures, *Acta Mater.* 49 (2001) 1035–1040.
- [17] C. Pozrikidis, *An Introduction to Grids, Graphs, and Networks*, Oxford University Press, 2014.
- [18] Y. Jiang, Q. Wang, Highly-stretchable 3D-architected Mechanical Metamaterials, *Sci. Rep.* 6 (2016) 34147. <http://dx.doi.org/10.1038/srep34147>.
- [19] J. Paulose, A.S. Meeussen, V. Vitelli, Selective buckling via states of self-stress in topological metamaterials, *Proc. Natl. Acad. Sci.* 112 (2015) 7639–7644.
- [20] M. Kadic, T. Bückmann, N. Stenger, M. Thiel, M. Wegener, On the practicability of pentamode mechanical metamaterials, *Appl. Phys. Lett.* 100 (2012) 191901. <http://dx.doi.org/10.1063/1.4709436>.
- [21] M. Kadic, T. Bückmann, R. Schittny, M. Wegener, On anisotropic versions of three-dimensional pentamode metamaterials, *New J. Phys.* 15 (2013) 023029.
- [22] K.C. Cheung, N. Gershenfeld, Reversibly assembled cellular composite materials science, *AAAS* 341 (2013) 1219–1221.
- [23] G. Gurtner, M. Durand, Structural properties of stiff elastic networks, *Europhys. Lett.* 87 (2009) 24001. <http://dx.doi.org/10.1209/0295-5075/87/24001>.
- [24] Y.C. Fung, *Foundations of Solid Mechanics*, Prentice Hall International, 1965.
- [25] M.E. Gurtin, in: C.A. Truesdell (Ed.), *The Linear Theory of Elasticity*, *Handbuch Der Physik*, vol. 6a/2, Springer, Berlin Heidelberg, 1972, pp. 1–295.
- [26] A.E.H. Love, *A Treatise on the Mathematical Theory of Elasticity*, fourth ed., University Press, Cambridge, UK, 1927.
- [27] A.H. Nayfeh, P.F. Pai, *Linear and Nonlinear Structural Mechanics*, in: *Wiley Series in Nonlinear Science*, Wiley, 2004.
- [28] H. Lee, J. Zhang, H. Jiang, N.X. Fang, Prescribed pattern transformation in swelling gel tubes by elastic instability, *Phys. Rev. Lett.* 108 (2012) 214304.